DTU Library

Spectroscopic Fingerprinting of Organic Material Extracted from Tight Chalk Core Samples of the North Sea

Mihrin, Dmytro; Li, Ming; Sánchez, Maria Alejandra; Hoeck, Casper; Larsen, René Wugt; Feilberg, Karen Louise

Published in:
ACS Omega

Link to article, DOI:
10.1021/acsomega.0c04431

Publication date:
2020

Document Version
Publisher's PDF, also known as Version of record

Citation (APA):
Mihrin, D., Li, M., Sánchez, M. A., Hoeck, C., Larsen, R. W., & Feilberg, K. L. (2020). Spectroscopic Fingerprinting of Organic Material Extracted from Tight Chalk Core Samples of the North Sea. *ACS Omega*, *5*(49), 31753–31764. https://doi.org/10.1021/acsomega.0c04431

ACS OMEGA

http://pubs.acs.org/journal/acsodf Article

Spectroscopic Fingerprinting of Organic Material Extracted from Tight Chalk Core Samples of the North Sea

Dmytro Mihrin, Ming Li, M. Alejandra Sánchez, Casper Hoeck, René Wugt Larsen, and Karen Louise Feilberg*

Cite This: *ACS Omega* 2020, 5, 31753–31764 Read Online

ACCESS | Metrics & More | Article Recommendations | Supporting Information

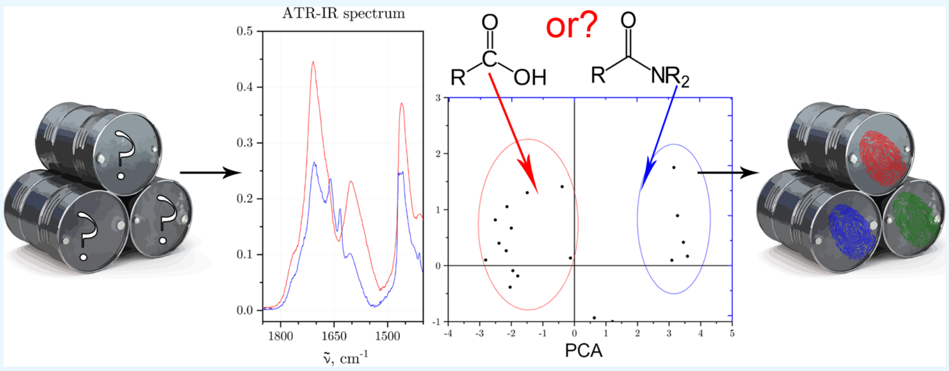

ABSTRACT: The detailed chemical composition of crude oil in subsurface reservoirs provides important information about reservoir connectivity and can potentially play a very important role for the understanding of recovery processes. Relying on studying produced oil samples alone to understand the rock-fluid and fluid−fluid interactions is insufficient as the heavier polar components may be retained by tight reservoirs and not produced. These heavy and polar compounds that constitute the resin and asphaltene fractions of crude oil are typically present in low concentrations and yet are determining for the physical−chemical properties of the oil because of their polarity. In order to obtain a fingerprint analysis of oils including polar compounds from different wells, the oil content of drill cores has been extracted and analyzed. Infrared spectroscopy has been used to perform chemical fingerprinting of the oil extracted from drill cores sampled in different geographical locations of the Danish North Sea. Statistical analysis has been employed to identify the chemical differences within the sample set and explore the link between chemical composition and geographic location of the sample. A principal component analysis, based on spectral peak fitting in the 1800−1400 cm^{-1} range, has allowed for statistical grouping of the samples and identified the primary chemical feature characteristic of these groups. Statistically significant differences in the quantities of polar oxygen- and nitrogen-containing compounds were found between the oil wells. The results of this analysis have been used as guidelines and reference to establish an express statistical approach based on the full-range infrared spectra for a further expansion of the sample set. The chemical information presented in this work is discussed in relation to oil fingerprinting and geochemical analysis.

1. INTRODUCTION

Infrared spectroscopy is a fast and robust screening method to perform fingerprinting of the oil samples[1,2] and uncover the chemical differences. The approach is well-fitting for direct observation of the polar constituents of crude oil because the corresponding functional groups display specific vibrational spectral features.[3] However, the method benefits from preliminary chromatographic separation of the sample analogous to the SARA[4,5] procedure, namely, to remove nonpolar fractions, that are better analyzed using, for example, gas chromatography (GC).[6] The present study is composed of two parts. In the first part, tight chalk drill core samples from Dan, Halfdan, and Kraka fields are studied. This sample set is used to set up the analysis method and focus on characterizing the chemical differences between the wells, particularly associated with the O- and N-containing polar molecules, and whether statistically significant correlations could be extracted from the infrared spectra. In the second part of the study, a set of tight chalk drill cores sampled in different geographical locations in Valdemar field are investigated. This study is focused on application of the established method to

Received: September 10, 2020
Accepted: November 13, 2020
Published: November 30, 2020

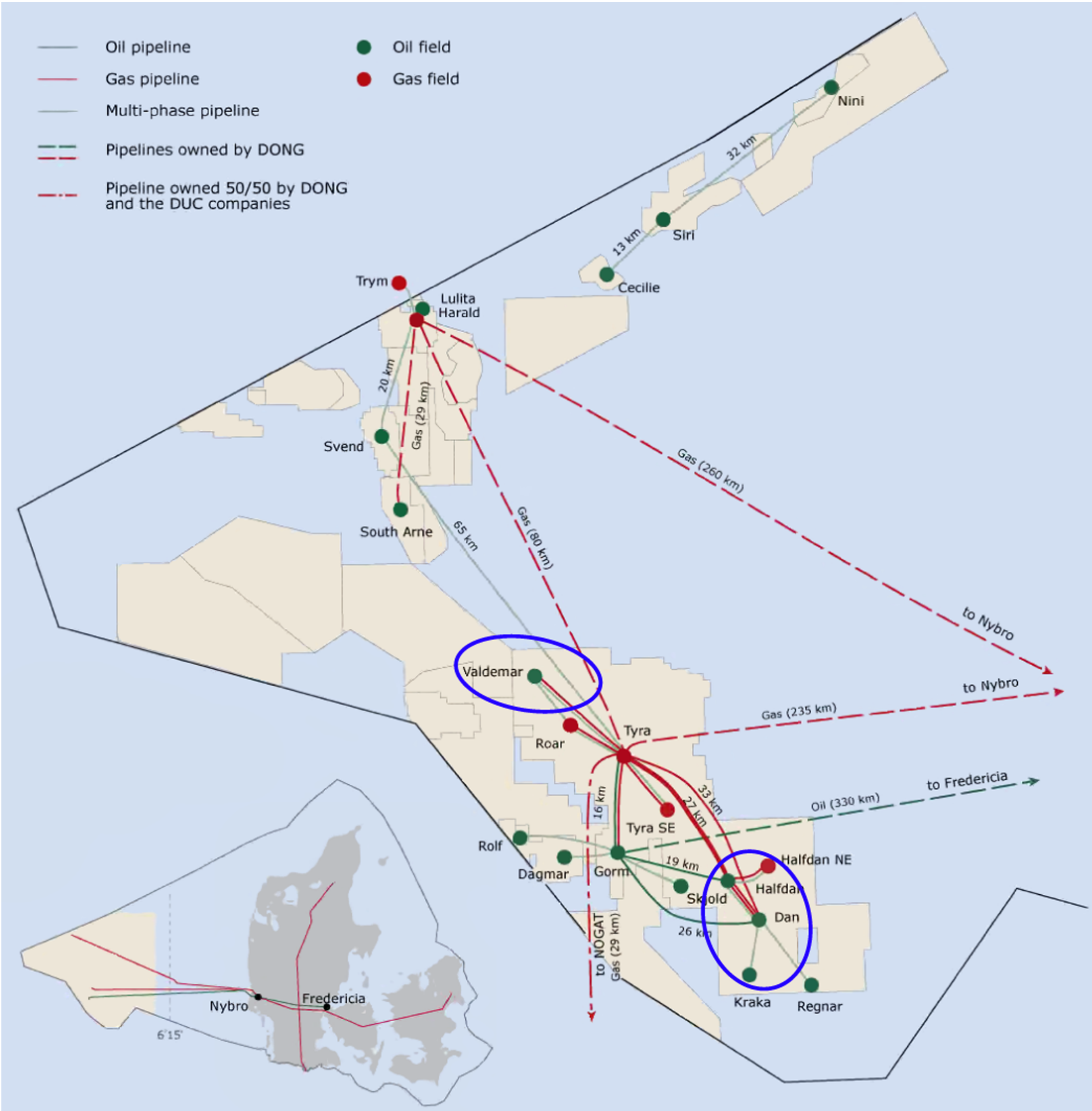

Figure 1. Map of the production facilities in the Danish North Sea (reprinted with permission from the "Danmarks olie-og gasproduktion 2012" report. Copyright Energistyrelsen, 2012.[19]). The fields in the South North Sea and the Valdemar field, where the tight chalk drill cores were obtained, are circled in blue.

uncover the variation in chemistry across the wells in the Valdemar field.

Detailed oil characterization and understanding local variations has wide implications within oil and gas. The nonideality of fluid properties of petroleum cause pre-established flow modes to be heavily composition-dependent.[7] The sample systems used for their construction are also a crude approximation of the fluid composition that will occur practically during production at various points in time.[8] Specifically, as the flooding fluid is altered, different compound classes will be mobilized and contribute to the nonideal behavior of the flowing liquid. The polar components of the oil are especially important, as they are surface active tend to concentrate on the oil/brine interface,[9,10] affecting interfacial tension, emulsification potential while also being capable of adhering to the reservoir rock surfaces in competition with water molecules.[11] Detailed studies of the first layer of oil adsorbed to rock surfaces show that the polar groups of these compounds attach strongly, leaving the hydrocarbon tail of the adsorbed molecule facing outwards.[12] The hydrocarbon tail can be involved in noncovalent molecular association by means of nonspecific van der Waals forces and hydrogen bonding, defining the physico-chemical properties of that surface, for example, wettability. These polar compounds are often not characterized by most conventional petroleum characterization techniques, where the focus is on the main saturated and aromatic constituents, but could have particularly dramatic impact on understanding the chemical behavior of the oil. In tight and highly porous chalk reservoirs, with reactive calcite surfaces, such a description of the detailed oil chemistry is needed to understand the observed mixed-wet behavior of the reservoirs. The chemical interactions between crude oil and production chemicals also depend on the most reactive and

https://dx.doi.org/10.1021/acsomega.0c04431
ACS Omega 2020, 5, 31753−31764

polar compounds, and a detailed chemical description can help target treatment additives to the reservoir.

The complex interplay of brine, oil, and rock surfaces can vary depending on the conditions in a particular reservoir. One approach to advanced oil recovery is the attempt to alter the wettability of the rock,[13,14] for example, by changing the ionic composition of the injection water in water-flooded reservoirs or by introduction of surfactants to the injection water.[15,16] However, the precise physical and chemical mechanisms that govern the wettability changes of the rock that appear linked to chemical changes in the injection water are still not fully understood. Because of the complex nature and size of oil reservoirs, accurate field scale simulations of recovery processes are computationally challenging.[17] Water-based oil recovery methods have been studied for application to many different types of reservoirs and have seen application in both carbonate and sandstone reservoirs to maximize the performance of the wells and sweep efficiency. Seawater injection is often applied to improve recovery and provide pressure support of the reservoir. Enhanced methods, such as modified salinity flooding and/or solvent flooding, can then potentially be employed in order to optimize recovery, although the mechanisms behind the modified salinity effects have not been well understood. However, it is certain that one of the keys to this phenomenon is the fluid−fluid interactions between the oil in the reservoir and the injection liquid as well as the impact the flooding has on the chemistry of produced fluid.[18]

2. GEOGRAPHIC ORIGIN OF SAMPLES

The samples originate from the Dan, Halfdan, Kraka, and Valdemar fields (Figure 1) and were all provided by Total E&P Danmark (formerly Maersk Oil and Gas). Kraka was the first of the chalk fields discovered in the Danish North Sea in 1966 and was put into production in 1986. Halfdan, Dan, and Kraka are located in the Southern part of the Danish Underground Consortium sector, and Valdemar is located near the central part. Kraka and Valdemar are to date not water-flooded, whereas Dan has been water-flooded after initial production and Halfdan has been water-flooded from the start of production.

The samples for this characterization study are the original drill core from the Dan, Halfdan, Kraka, and Valdemar fields (Figure 1).[19] The Dan, Halfdan, and Kraka fields are closely related by geology and fluid migration. The producing wells in Dan and Halfdan are located in the Maastrichtian chalk (Tor formation) and the Kraka wells are located in the Danian chalk (Ekofisk formation), both being in the upper Cretaceous. The current reservoir conditions after 15−25 years of production for these fields are temperatures in the range $T = 60 - 70$ °C and pressures in the range ∼160−170 bar. The Valdemar field produces from wells in the lower Cretaceous, mainly the Tuxen formation, with average reservoir conditions of $T = 90$ °C and the pressure of 300 bar. The drill core samples were selected on the basis of geological position and availability of core material to get samples from as wide a geological area within the four fields as possible. The core samples for chemical analysis were taken as 20−40 g miniplugs drilled from the center of the original drill cores to avoid the material that has been exposed directly to atmosphere, hydrocarbon-based drilling liquids, and mechanical influence. The influence of the atmosphere is assumed to be limited because of the low permeability of the rock material. The Tor chalk has permeabilities around K = 0.5−2 mD, while the Valdemar chalk has extremely low permeability, K = 0.08−0.12 mD. The complete list of samples is given in Table 1.

Table 1. List of Drill Core Samples Originating from the Valdemar Field and Fields in the South North Sea (Dan, Halfdan, and Kraka) Included in This Study[a]

Valdemar		South North Sea	
Well Name	Depth/ft	Well Name	Depth/ft
North Jens	7453	MFA14	7648
	7462	A6I	9527
	7479		9515
	7487		9530
	7499	MFB7	7373
	7525		7377
			7560
Valdemar 2H	9975-78	Nana1XP	6990
	9978-81		7226
	9981−84 S1		7006
	9981−84 S2	MFA4	7788
	9999−10021 S1		
	9999−10021 S2		
Valdemar 2P	7525		
	7688		
	7579		
	7713		
Bo-2X	7063		
	7844		
	7857		
	7868		
	7886		
	7901		

[a]When closely located samples from the same depth were used, the samples are indicated with a comment. Samples obtained from the same drill core in different areas are denoted as S1,2.

3. EXPERIMENTAL METHODS

The crude oil deposited in the tight chalk drill core sample material has been analyzed by means of the initial solvent extraction (Section 3.1), followed by further chromatographic separation of the solvent extracts by solid-phase extraction (SPE) methods (Section 3.2) before the final spectroscopic

Table 2. Solvent Elution Scheme for the Developed SPE Procedure of Core Sample Extracts on NH_2, SCX, and Silica Columns (Si), and the General Chemical Composition of the Different Fractions Labeled A to E[a][20,21]

		Solid Phase		
Cut	Chemical Composition	NH_2	SCX	Si
A	aliphatics, light aromatics	heptane		
B	polyaromatics	20% toluene/80% heptane		
C	asphaltenes, polar	toluene		
D	asphaltenes, acids, amides	20% methanol/80% toluene		
E	acids/primary amides	15% methanol	15% methanol	no fraction
		80% toluene	80% toluene	collected
		5% formic acid	5% pyridine	

[a]Values expressed as % V/V.

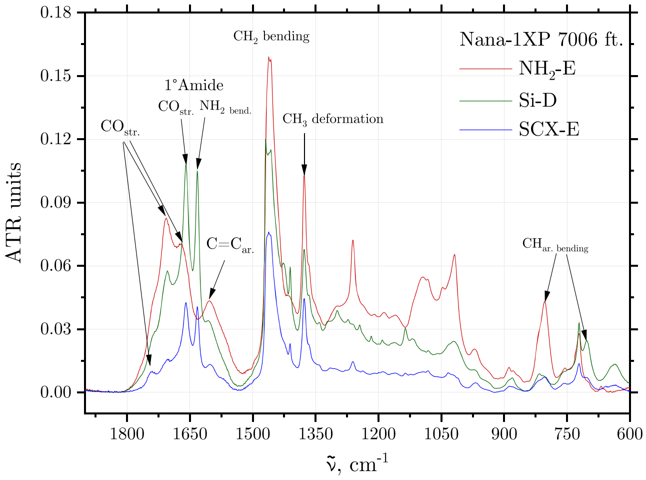

Figure 2. Infrared spectra in the 1900−600 cm^{-1} range for the last fractions obtained on a silica column, NH_2, and SCX columns for the Nana-1XP drill core extract. The most important vibrational band assignments are indicated in the spectrum.

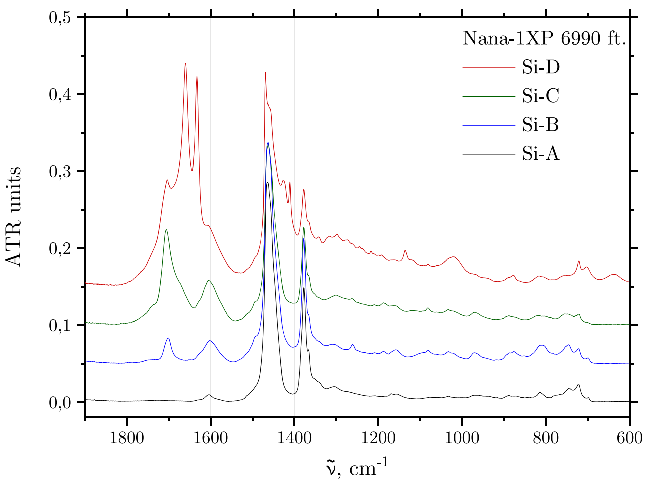

Figure 3. Infrared spectra in the 1900−600 cm^{-1} range for the A−D fractions obtained on a silica column for the Nana-1XP drill core extract.

analysis by attenuated-total-reflection (ATR) Fourier transform infrared (FTIR) spectroscopy (Section 3.3).

3.1. Initial Solvent Extraction. The central parts of a tight chalk cores, which are less likely to exhibit artifacts related to drilling mud or large heterogeneous sections, are first cleaved out and grounded in a mortar to obtain a semifine uniform powder and subsequently stirred. Then, an approximately 1 g of the sample is transferred into a separate vial, and 4 mL of dichloromethane is added. The mixture is stirred on a shaker for an hour and subsequently centrifuged. The supernatant is transferred into a different vial, and another portion of dichloromethane is added to the powder and shaken overnight. The two extracts are merged and dried under a gentle gas stream of nitrogen to estimate the mass of the extracted oil. Based on the measured mass, the sample is then redissolved in an appropriate volume of dichloromethane and a portion of that solution is transferred into an HPLC vial. The amount transferred is chosen to obtain a quantity of material suitable for loading of a 500 mg SPE column and is typically in the range from 20 to 30 mg. The sample is then dried and redissolved in 0.5 mL of *n*-heptane, aided by sonication.

3.2. Solid-Phase Extraction. The SPE column is conditioned with 3 mL of dichloromethane and equilibrated with 6 mL of heptane. The sample is loaded onto the column, and the vial is then washed by another 0.5 mL of heptane. In some cases, the sample is rich in heptane-insoluble material that might stick to the glass surface. In these cases, the residue was dissolved in the heptane−toluene mixture, used in the second round of elution and is loaded when the column wash is changed to that solvent. Two column volumes of the eluent are added at each step, amounting to 4 mL, with four fractions produced. Elution is performed by gravity, with the fractions collected in 8 mL glass vials. The fractions are subsequently dried under the stream of nitrogen in a sample concentrator apparatus, where the vial is placed in a cast aluminum block heated to 35 °C, and the gas is delivered through the needle placed about a centimeter above level of the liquid.

The purpose of chemical separation of the sample is to produce fractions defined by the chemical properties of the components. The present study is primarily focused on the polar compounds adsorbed on the chalk surface. However, the organic material extracted from the core contains substantial amount of heavy nonpolar compounds. After separation on the silica column as described above, the D-fraction constitutes anywhere from 15 to 42% of the total mass. The heptane-soluble components of the extract add up to ca. 50−60% of the total mass of the extract. The presence of nonpolar compounds effectively dilutes the sample, reducing the signal from the polar compounds.

The column and the elution procedure was selected to provide the most effective separation of the polar compounds, while not leaving any sample material behind. The three column types were tested during the method development, namely, the discovery amine (NH_2), strong cation exchange (SCX), and silica (Si) columns (Supelco). The eluents used for each cut and their approximate composition are given in Table 2.

The potential benefit of the SCX and amine columns is the ability to additionally separate the acidic components from the basic. To elute the adsorbed material, an additional step after the D fraction using formic acid or pyridine added to the eluent was used for the NH_2 and SCX columns, respectively. The last fraction of the NH_2 column contains mostly acidic components, while the SCX column shows only small traces of carbonyl-containing compounds but yields all of the amides. The silica column contains features of both in the proportions closer to which these compounds are present in the sample. Because all of the important features are present in the silica column and sufficient separation is achieved, it was decided to use this column for the routine measurements to form a large sample set. The reasoning is particularly reinforced by the issues that appeared in some cases when more specialized columns were used, particularly with the SCX solid phase. Because samples have different chemical composition and more importantly different distribution of the relative fraction masses, a proper elution of the heavier components from the column was often problematic. The interaction of the column material with the sample and the eluent at the C, D, or E fractions caused noticeable column bleed and clogging. The silica column did not show any of these issues and is chemically stable. The elution takes approximately 30−40 min for each fraction. In some cases, the last fraction may leave a visible residue after the defined volume of the eluent has been passed. In this case, an additional eluent or a stronger solvent can be introduced without the risk of damaging the column. Another concern regarding the eluent, primarily from the perspective of convenience, is that the mixtures for the E fractions needs to be prepared as close to use as possible, for each analysis, because of the formation of emulsions after several hours.

3.3. ATR-FTIR Spectroscopy. The ATR-FTIR spectra have been obtained employing a Bruker Vertex 80v vacuum FTIR spectrometer equipped with a Bruker single-reflection diamond ATR accessory. The spectrometer was equipped with a liquid nitrogen-cooled broadband HgCdTe detector, a Ge on KBr beam splitter, and an air-cooled globar radiation source. A spectral resolution of 1 cm^{-1} was employed for all recordings, and blocks of 500 scans were obtained for both the sample and background (clean diamond crystal before and after sample recordings) interferograms. The generated absorbance spectra were all cut in the standard 4000−500 cm^{-1} spectral region, and proper baselines were generated with a single iteration of concave rubber-band correction. Advanced ATR corrections were finally applied to compensate for the wavelength dependence of the penetration depth using standard parameters of the OPUS software.[22]

For the ATR measurements, the fractions are dissolved in small quantities of the respective elution solvent, to be transferred onto the ATR crystal. The amount of the solvent was roughly one drop per 0.5 mg of matter. The solution was collected with a glass pipette and placed on the ATR crystal. The spectrometer was then evacuated, drying the sample of any traces of the solvent and moisture, which was ensured by monitoring the change of the infrared spectra over time.

The ATR spectra obtained for the last fraction for each respective column for an example core extract are presented in Figure 2, illustrating the relative abundance of acids and amides identified by their carbonyl stretching bands near 1700 cm^{-1}. Several representative spectra of each fraction obtained on the silica column are shown in Figure 3. The A fraction is primarily composed of aliphatic hydrocarbons with only a trace of aromatics. The B fraction contains nonpolar compounds with few fused aromatic rings and small amounts of carbonyl-containing compounds,[20] that likely do not form strong hydrogen bonds to the silica surface, such as ketones. The A and B fractions are expected to have substantial overlap,[23] as there is no specific difference in interaction with the stationary phase, and such mixtures are best measured with a dedicated column[21] or by GC. In the C fraction, polar compounds elute, while amide-containing components are seen to escape in the D fraction. The last fraction contains components that have multiple carboxylic or amide groups. More detailed vibrational band assignments are given in the following section concerned with the aim to establish statistical correlations between observed spectral signatures and the different well samples.

4. STATISTICAL METHOD DEVELOPMENT

4.1. Principal Component Analysis Approaches Based on Curve Fitting and Full-Range Spectra. The generated infrared spectra of the crude oil residues are very rich in chemical information even after the separation procedures. The multiple distinct infrared spectral features provide qualitative information about the specific functional groups of the abundant chemical compounds. The applied ATR correction procedures furthermore ensure a direct proportional relationship between observed band intensity and the corresponding abundance of the absorbing species in

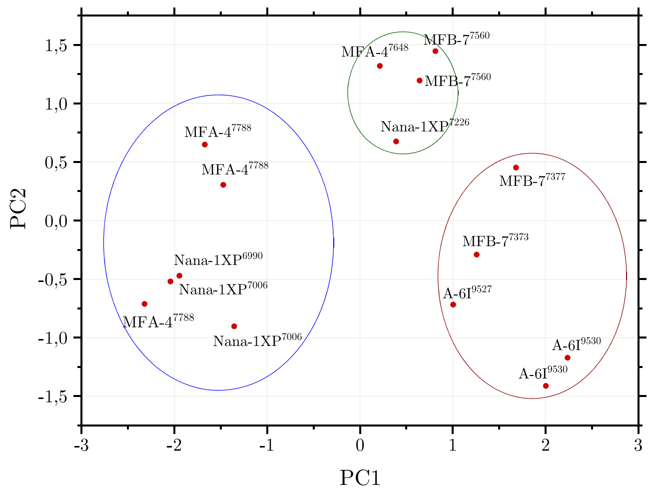

Figure 4. Score plot of the PCA of the drill core samples from the Dan, Halfdan, and Kraka fields employing the spectral peak-fitting approach in the fingerprint range (1800−500 cm^{-1}). The colored circles indicate the suggested groupings of the samples.

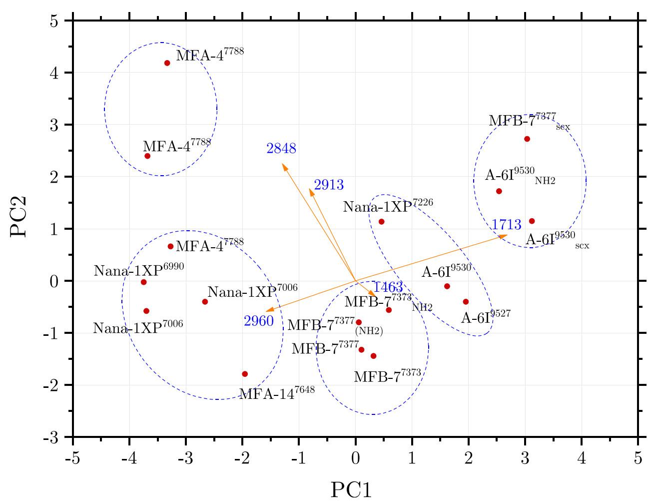

Figure 5. Biplot of the PCA of the drill core samples from the Dan, Halfdan, and Kraka fields performed directly on the selected ranges (3800−2700 and 1850−600 cm^{-1}) infrared spectra of the fractions obtained on the silica columns. The orange vectors on the plot represent the dominant contributions to the PCs. The groups were determined from a *K*-means cluster analysis.

the framework of Lambert−Beer's law. The normalization of the absolute ATR intensity scale based on isolated spectral features for the most abundant hydrocarbons then provides information about the relative abundance of the less abundant but important polar constituents. In the statistical analysis presented here, the complete set of infrared spectra has been normalized with respect to the isolated vibrational band around 1450 cm^{-1} associated with the CH_2 bending modes of aliphatic hydrocarbons.

The major quality for a suitable statistical method is to provide as much chemical meaningful information from the experimental data. The aim is to achieve statistically significant results concerned with both the nature and relative abundance of polar compounds for a large array of core samples in a robust and fast manner and preferably by the use of an automated mathematical approach. The principal component analysis (PCA) approach is a widely applicable technique

https://dx.doi.org/10.1021/acsomega.0c04431
ACS Omega 2020, 5, 31753−31764

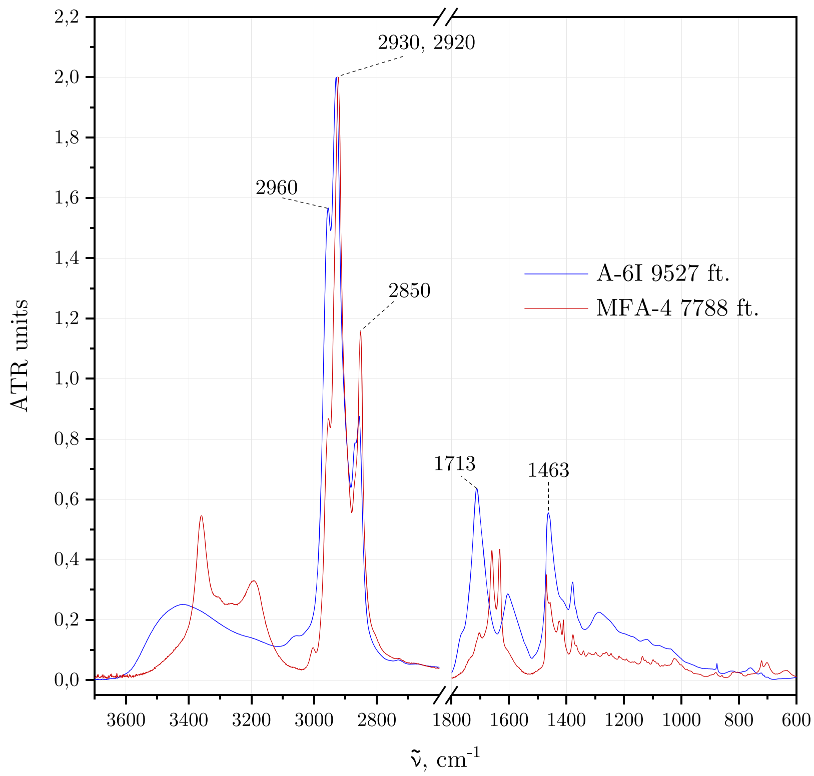

Figure 6. Full-range (3800−600 cm^{-1}) infrared spectra of the D fractions obtained from the drill core samples from the Dan, Halfdan, and Kraka fields on the opposite sides of the PCA biplot, calculated directly from the spectral data (Figure 5). The peaks corresponding to the dominant contributions to the first two PCs are indicated. The axis break excludes the part of the spectrum where the diamond artifact is present.

where the goal is to find a lower-dimensional representation of a high-dimensional data set.[24] In short, PCA can reduce the dimensionality of a data set, while minimizing the loss of variability or statistical information in the samples. It is a systematized way to transform high-dimensional features into principal components (PCs) (new features) and group similar data sets. Thereby, PCA is suitable to find unlabeled clustering and recognize the patterns of groups.[25−27]

Two complementary PCA approaches have been investigated in the present work. The first PCA approach involves spectral peak curve fitting procedures to obtain the areas, intensities, positions, and widths of distinct assigned bands as variables for the analysis. Second, the full data points from the raw infrared spectra are employed directly with high dimension variables. The former approach has the advantage of starting out with lower dimension variables that have clear physical meanings and is less susceptible to the noise and spectral interference in the raw complete data sets. The disadvantage is the requirement of pre-established sets of vibrational assigned peaks to be fitted to each spectrum, regardless of the chemical composition of the samples. This may become a challenge as relevant spectral features often overlap for complex oil samples, making properly distinguishing between them and finding exact peak positions and areas very hard without manually introducing fitting constraints. Most of the time to achieve a satisfactory degree of consistency and reliability, peak fitting has to be done manually or the result from automated fitting should be carefully reviewed. This is rather time-consuming and restricts the number of samples to be processed by this curve-fitting procedure. The curve fitting analysis was carried out in the 1800−1500 cm^{-1} spectral range with Voigt band profiles employing the Fityk[28] program. The curve fitted band areas are then used as inputs for the PCA module of the Origin[29] software package.

The second statistical approach has the benefit of much faster processing times and excludes human error or bias from the analysis. On the other hand, this method has to deal with a large number of variables with multiple dependencies, of which one of the more challenging ones to elucidate is the overlapping of individual vibrational bands. This is because it by default assigns each point and its intensity as a feature group. As a consequence, the statistical results can be affected by equipment noise and explains why spectral smoothing procedures are important in the data preparation process. In this work, the PCA was carried out using an in-house developed program working on the full-range infrared spectra after applying baseline and ATR corrections.

The main goal of the present work is to establish a statistical approach to process spectroscopic data obtained from the drill core samples and elucidate the parameters that best describe the chemical differences between the wells located in different geographical points. The second objective is to validate the use of the express method to analyze the core samples and apply this faster PCA approach to understand the difference in chemistry in the wells of the Valdemar field and its link to crude oil production.

4.2. PCA of Samples from the Dan, Halfdan, and Kraka Fields. The samples from the Dan, Halfdan, and Kraka fields have been used to test and optimize both experimental and statistical methods. In Figure 4, the results from the PCA based on spectral fitting in the fingerprint region (1800−600 cm^{-1}) are shown. The variables were collected from all the three column types and replicates were used to assess the uncertainty of the analysis.

https://dx.doi.org/10.1021/acsomega.0c04431
ACS Omega 2020, 5, 31753−31764

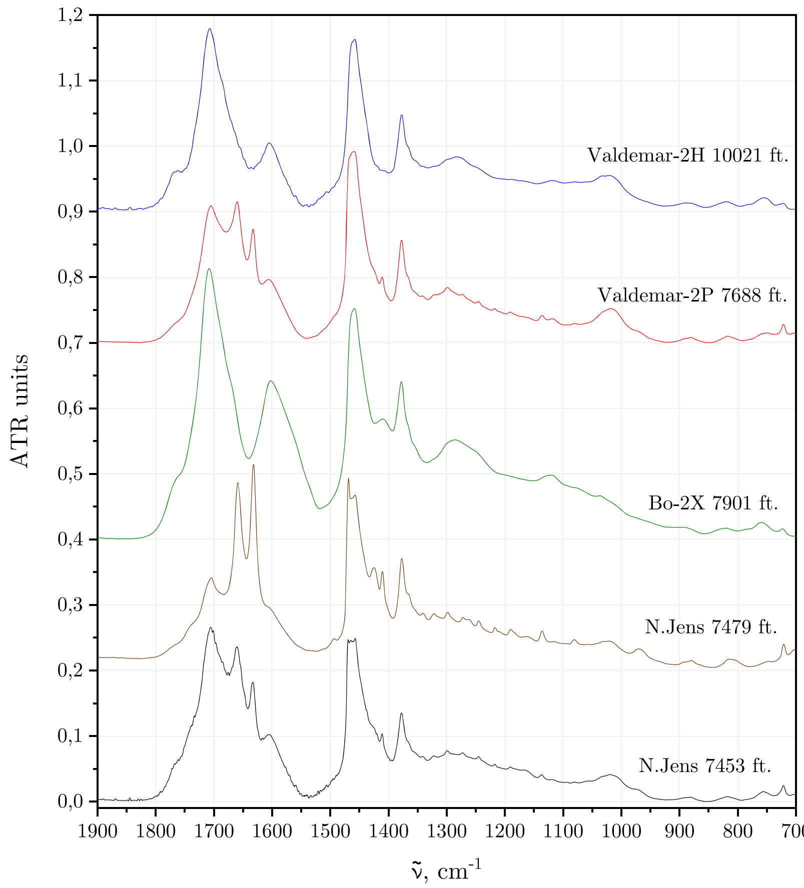

Figure 7. Infrared spectra of the D fractions separated on a silica SPE column for the samples extracted from the drill cores obtained in the Valdemar field.

The samples form three distinctive groups based on the first two PCs. The first PC describes the acid/amide mutual ratio, with samples on the left containing mostly amides, while the ones on the right are rich in carboxylic acids. The second PC is primarily affected by the intensity of the aromatic C=C peak and the sub-band with a maximum near 1680 cm^{-1}.

Figure 5 shows the second approach to the PCA with the same sample set. For this case, data from the four fractions of each sample were used for the analysis, and the full recorded spectral range (excluding the 1850 to 2700 cm^{-1} range) was included. The PCA results were compared with *K*-means (n = 5) methods. Overall, the distribution of samples qualitatively agrees with the results of the first approach, with most of the samples maintaining proximities illustrated in the previous figure. For example, the MFB samples group with A-6I and the MFA group with the Nana-1XP wells. However, the indicated loadings suggest that the C−H stretching and bending bands are contributing significantly to the variance of the sample set. Still, the carbonyl stretching band has the highest absolute contribution and is the dominant component of the first PC. This is the reason that most correlations along the first PCs are very similar, while distribution by the second PC is different in many cases. This is to be expected as additional information is introduced into the analysis.

Figure 6 shows the overlay of the two spectra on the opposite sides of both PCs. The features contributing the most to the PCs are marked on the figure. Evidently, the most distinguishing features are related to the ratios of the stretching modes, that is, branching of the carbon skeleton, and comparative abundance of the oxygen-containing compounds, presented by the carbonyl stretching band at 1713 cm^{-1} with respect to the CH bending mode. Surprisingly, the absorption of the amide compounds are not among the first five major descriptors, even though the groupings are in good agreement with the fitting-based method.

The overall conclusion regarding this set is that samples are sufficiently differentiated based on the chromatographic separation on a silica column. The preliminary results from the PCA carried out for this set shows that generally the same groupings can be obtained by using either the full spectral range or just the fingerprint region of the infrared spectra.

Apart from the benefit of being fast, the analysis based on full-range spectral data points directly has extra advantages. Using the C−H stretching bands can be quite challenging in practice, as polar fractions contain carboxylic groups, that in turn produce a broad and strong absorption in the 2800−3600 cm^{-1} related to the O−H stretching band of the strongly interacting acid molecules, introducing a baseline tilt under the C−H stretching band. This is a major problem for peak-fitting procedures in this range, but likely can be easily addressed with a point-by-point approach as it could take into account the intensity contribution from the O−H stretching band.

5. RESULTS AND DISCUSSION

The samples from the Valdemar field were analyzed using the finalized method employing only the silica column with four fractions produced, and both PCA approaches were employed. The spectral fitting procedure was performed on the D fraction

https://dx.doi.org/10.1021/acsomega.0c04431
ACS Omega 2020, 5, 31753−31764

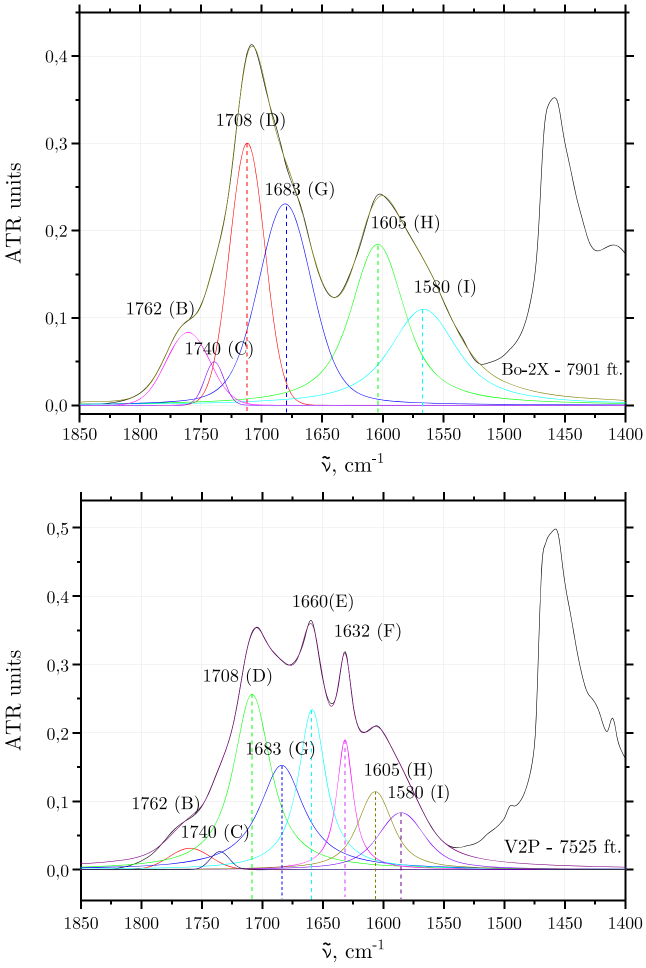

Figure 8. Example of the spectral peak-fitting procedure performed on the basis for the PCA of the crude oil extracts. The average peak positions and the attributed notations for Figure 9 are indicated next to the corresponding peaks.

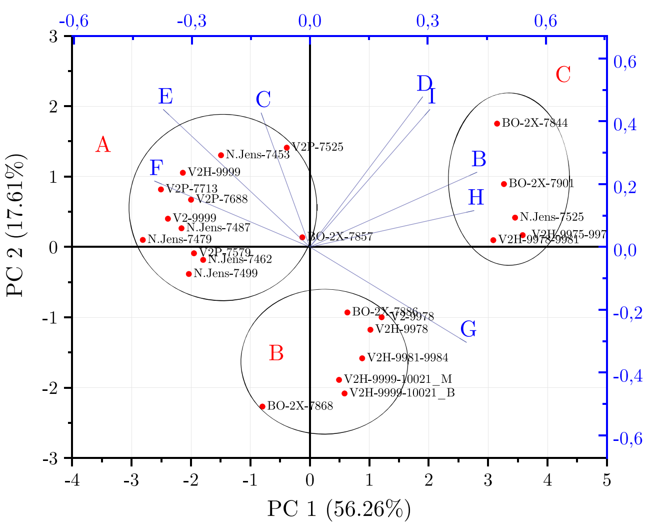

Figure 9. Biplot of the PCA performed for the D fractions of the drill core extracts from the Valdemar field. The blue vectors indicate contribution of the variables, measured from the spectral fitting approach (Figure 8), to the first two PCs. Based on the resulting scores, the samples are grouped into the three groups indicated by the circles.

only, in the 1800−1500 cm^{-1} spectral range, with the purpose to explore potential significantly different abundances of polar compounds. The direct PCA of the raw infrared spectra was performed on a combination of the C and D fractions, as this approach appeared to produce the most consistent grouping of samples. On the contrary, the A and B fractions did not show any clear correlation and the variance was comparable to the experimental noise.

Examples of the infrared spectra of the D fractions for the samples originating from the Valdemar field are given in Figure 7. A significant variance in the vibrational features is observed for the samples studied. By observation, it appears that acids, amides and aromatics are abundant in vastly varying amounts with respect to one another.

A few examples of the peak-fitting results used to produce PCA plots are given in Figure 8. In the most simple case, the spectrum in the desired range is presented by two strong peaks attributed to the carbonyl stretching and the aromatic C═C stretching vibrations. Most of the spectra also show a very distinct extra feature on the main carbonyl peak near 1760 cm^{-1} (B) most likely attributable to another carbonyl compound. On careful inspection of all the samples side-by-side, changes in the peak intensity allow us to uncover additional spectral features. These are bands at 1683 cm^{-1} (G), this band appears as a shoulder on the strong carbonyl stretching band, often almost entirely concealed by it, and another band with a center close to 1580 cm^{-1} (I). The latter is attributed to an aromatic vibration like the 1605 cm^{-1} (H) band, or potentially, it could be associated with another carbonyl-containing compound class.

The band at 1683 cm^{-1} (G) could potentially be attributed to the C═O stretch in the secondary amide group, quinones, or other carbonyl-containing compounds. The common appearance of the latter in some of the C fractions suggests that the respective compound class has weaker interaction with the silica surface. This feature has qualitative correlation with a signal at 3423 cm^{-1}, favoring the secondary amide assignment; however, this cannot be reliably concluded by means of FTIR alone. Last, a weak band near 1740 cm^{-1} (C) is observed as a shoulder on the main carbonyl stretching band. As this band is very weak, it only shows up clearly in a few observed samples, where the stronger bands obscuring it are smaller. Unfortunately, there is no clear information about the nature of this band, but because of the fact that it often appears as a distinct shoulder, it is necessary to include this to reduce the error associated with fitting other bands. Naturally, extra care has been taken to produce meaningful peak fits for the bands that are strongly overlapped in many samples, yet it should be noted that uncertainties associated with exact peak positions and areas are somewhat larger from sample to sample. The most important part of the method was to restrict the peak position to within 5 cm^{-1} of the average value observed, and the fits were reiterated several times.

The bottom spectrum shown in this figure illustrates a case where a detectable amount of primary amides is present in the sample. Two signals are characteristic of these compounds, assigned at 1660 (E) and 1632 cm^{-1} (F), for the C═O stretching and NH_2 bending bands, respectively.

The results of the PCA on the fittings are shown in Figure 9. Loadings vectors correspond to the assignments on Figure 8. Three groups can be obtained from the analysis. The main PC differentiates the samples based on the presence of primary amides (negative vectors E, F), acids, aromatics, or the G

https://dx.doi.org/10.1021/acsomega.0c04431
ACS Omega 2020, 5, 31753−31764

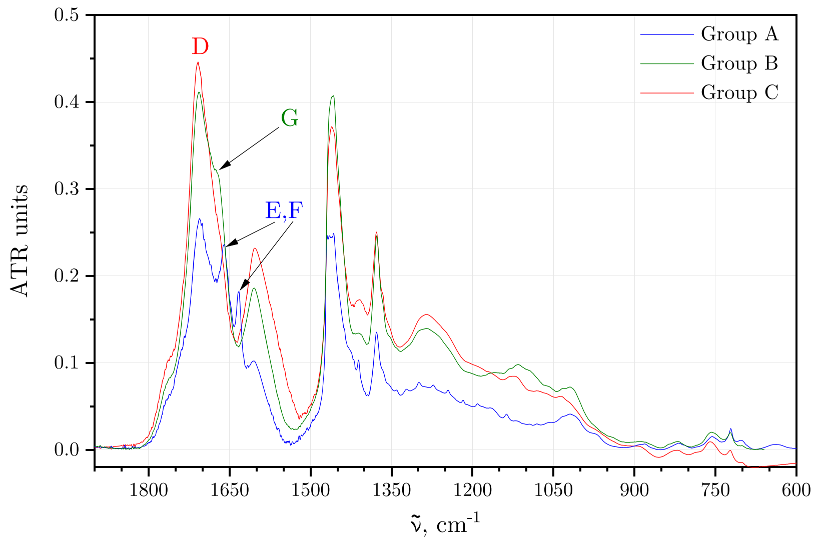

Figure 10. Infrared spectra of the example D fractions obtained from the samples in the three groups, as attributed from the fitting-based PCA approach. The primary differentiation features of the samples are indicated on the spectra as the corresponding peak assignments.

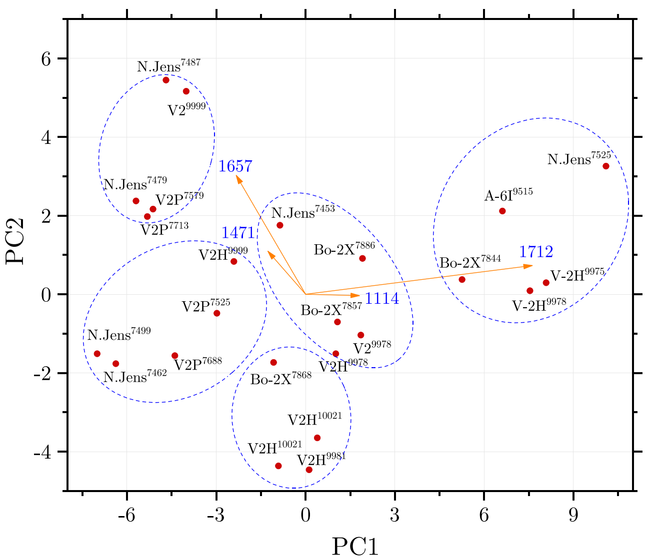

Figure 11. Biplot of the PCA of the drill core samples from the Valdemar field performed directly on the full-range infrared spectra of the fractions obtained on the silica columns. The orange vectors on the plot represent the dominant contributions to the PCs.

vector due to the band at 1683 cm^{-1} (positive contributions). Basically, without considering the second PC, the PCA scores show gradual distribution of samples from nitrogen-rich (amides) to oxygen-rich (acids). The second PC is responsible for establishing the third group alone, based on the value of the 1683 cm^{-1} feature (G). The G vector is anticorrelated with the D (acids), which could be in part because of overlap of these two peaks and the associated uncertainty in estimating the area of the peaks because they share the total model intensity to be reproduced. There appears to be general correlation between the D and I variables as well as between the B and H variables. Perhaps a more detailed investigation complemented by the GC−mass spectrometry techniques might reveal structural dependencies between these spectral features.

The examples of spectra measured for the representative samples from each group are shown in Figure 10. The sample from the amide group has a comparatively small amount of carboxylic acids, and the aromatic peak is weaker. The samples from the other two groups, on contrary, all show a strong acid band and the aromatic peak at 1600 cm^{-1}. Those two spectra are mostly differentiated by the evident shoulder of the 1683 cm^{-1} band and different ratios of the CH-bending/acid peaks.

The results of the analysis should be compared against the second approach to the PCA. Figure 11 shows the biplot of the direct PCA on the combined C and D fractions. The comparison of the two plots indicates that the results are similar between the two methods. The variables contributing to the PCs are also more consistent with the fitting method, as both the acid band and one of the amide bands are present among the highest contributors. Apart from those, the CH-bending band and a band in the fingerprint region are important to the score distribution. The samples can be categorized into three to five groups based on the *K*-means cluster analysis. Owing to the much larger number of variables, the overall distribution of the samples is more gradual compared to peak-fitting method. However, the most significant variation between the samples is properly captured and is not adulterated by the additional input, that is, North Jens-7479 and V2P-7579 are well grouped together in both methods, as well as acid-rich samples, for example, Bo-2X-7901, are well isolated.

The acids and amides present in the studied samples are some of the most interesting descriptors of the oil properties, as they are capable of engaging in strong intermolecular interactions. These compounds can be expected to bond to other acids and amides, ketones, and, most importantly, to the surface of the reservoir rock. The latter could be the defining factor to the mobility of the oil. Overall, it seems that the difference in these compound classes constitutes the most clear chemical difference in the chemistry of the wells investigated in this study obtained by infrared spectroscopy.

Figure 12 shows the results of quantification of the acid and the amide content in the extracted oil of the Valdemar drill core samples. The spectra were normalized by the CH-bending band, which should not have any overlap with the signals of the quantified groups and should also closely represent the reference for the total organic content measured in the ATR approach. This step is necessary, as the penetration depth of

https://dx.doi.org/10.1021/acsomega.0c04431
ACS Omega 2020, 5, 31753−31764

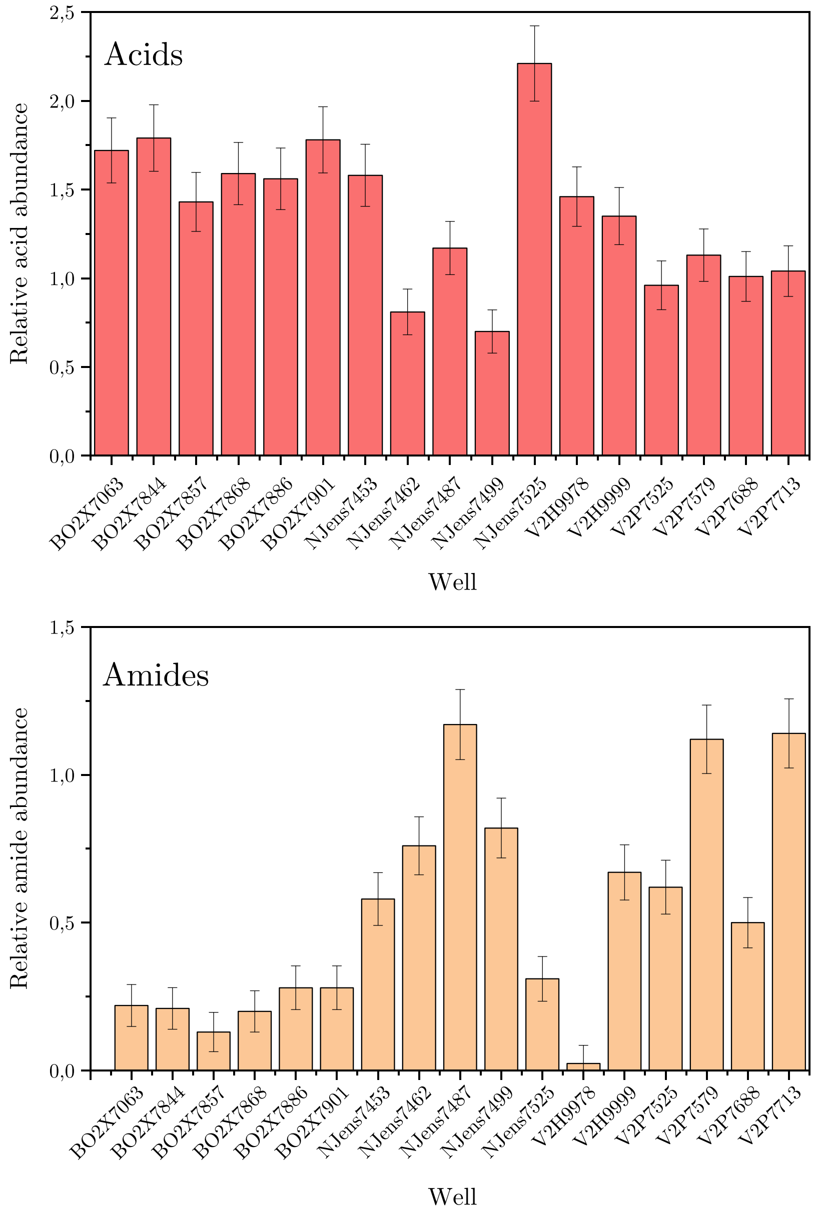

Figure 12. Relative abundances of acids (top) and primary amides (bottom) found in the oil wells of the Valdemar field based on their characteristic band intensities (the 1710 cm^{-1} band for acids and the 1632 cm^{-1} band for amides) in the spectra obtained for the D fraction of the extract. The spectra were all normalized by the CH_2 bending band intensity. Error bars are estimated as the standard deviation of the fitting.

the infrared beam in the ATR measurements is dependent on the refractive index of the sample and the wavelength of the light, and is ultimately limited by the thickness of the layer on the diamond crystal of the ATR module. For these reasons, a reference peak located as close as possible to the acid/amide bands is necessary for quantitative applications in our scenario.

The observation from these results is that the acids are present consistently in all of the samples and in significantly higher concentrations than found in any of the produced fluid fractions (Figure 13). The concentration of amides varies a lot more across the sample set. The quantity of amides in the Bo-2X wells is comparable to the uncertainty of the fitting procedure. It can be noticed that for most wells, the quantity of acids is inversely proportional to the quantity of amides, for example, all of the N. Jens wells are amide-rich and do not show as much acid content as Bo wells. It could be hypothesized that the approximately 3 times higher recovery factors observed for N. Jens and Valdemar wells (provided in private correspondence with the field operator) could be linked via the physical−chemical properties of the oil to the comparatively low abundance of acidic compounds in these wells. As amides form less stable intermolecular bonds, they might be expected to have less of an effect on fluid−fluid and fluid−rock interactions than acids.

An analytical investigation of well performance in several regions of the North Sea has been carried out by Nielsen *et al.*,[30] in which a link between the production of the wells and the presence of biomarkers, retene, and stereoisomers of steranes, was observed. This indicates an impact linked to the thermal maturity of oil. The chemical information obtained from tight chalk drill cores in this work is indented to be complemented by a future fingerprinting of produced oil samples from the fields, focused on recovering data on maturity, branching, and aromatic condensation.

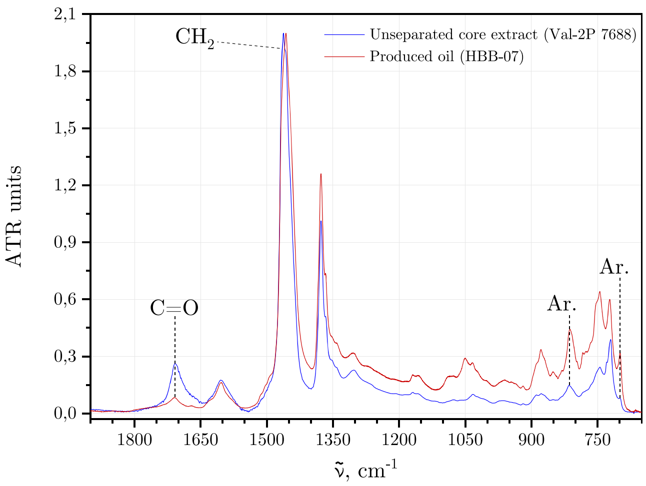

Figure 13. Comparison of the infrared spectra of a produced oil (HBB-07, red trace) and the drill core extract (blue) before the SPE procedure. The spectra are normalized by the CH_2-bending band intensity. The characteristic carbonyl stretching absorption is indicated on the graph, evidencing a significant difference in the acid content of the produced fluid and the deposited oil in a drill core before production.

6. CONCLUSIONS

The application of infrared spectroscopy has proven powerful and capable of distinguishing the chemical differences between crude oils from tight chalk cores sampled from different geographical locations. Statistically significant differences in the quantities of polar oxygen- and nitrogen-containing compounds, namely, carboxylic acids and amides, were found between the samples. The spectral data can be obtained routinely with the ATR method with less sample preparation and average analysis time than is usually the case with high-resolution GC techniques applied to heavy heteroatom compounds,[31] and the ATR method constitutes an excellent complementary technique to the latter. The samples show distinct intercorrelations and can be grouped with a PCA approach based on the observed infrared spectral signatures of polar compounds. The average composition of the drill core extracts is heavier and more rich in asphaltenes and resins than the produced oil. This suggests that the majority of the acidic compounds and amides are retained in the reservoir after the oil has been produced, and leaving this fraction behind has a detrimental impact on the recovery factor, as well as potentially negatively influencing the produced fluid flow throughout production. The strongest contributions in the statistical evaluation of the sample set come from the acid/amide ratio, with a comparatively higher amide presence found in the North Jens wells. The second PC of the set is mostly characterized by the ratio of 1683 cm^{-1} band and the respective features related to the primary amide content. The strong composition discrepancy between the retained material and the produced oil also creates some potential issues when changing the well flooding fluid without accounting for the changes in the chemical composition of the produced fluid.

■ ASSOCIATED CONTENT

Supporting Information

The Supporting Information is available free of charge at https://pubs.acs.org/doi/10.1021/acsomega.0c04431.

Full infrared spectra of the A–D fractions produced from representative samples from each of the groups defined in Figure 9, including *XY*-data files of the spectra (PDF)

■ AUTHOR INFORMATION

Corresponding Author

Karen Louise Feilberg − *Danish Hydrocarbon Research and Technology Centre, Technical University of Denmark, 2800 Kgs. Lyngby, Denmark;* orcid.org/0000-0001-7417-2380; Email: klfe@dtu.dk

Authors

Dmytro Mihrin − *Department of Chemistry and Danish Hydrocarbon Research and Technology Centre, Technical University of Denmark, 2800 Kgs. Lyngby, Denmark*

Ming Li − *Danish Hydrocarbon Research and Technology Centre, Technical University of Denmark, 2800 Kgs. Lyngby, Denmark*

M. Alejandra Sánchez − *Department of Chemistry, Technical University of Denmark, 2800 Kgs. Lyngby, Denmark*

Casper Hoeck − *Department of Chemistry, Technical University of Denmark, 2800 Kgs. Lyngby, Denmark*

René Wugt Larsen − *Department of Chemistry, Technical University of Denmark, 2800 Kgs. Lyngby, Denmark*

Complete contact information is available at: https://pubs.acs.org/10.1021/acsomega.0c04431

Notes

The authors declare no competing financial interest.

■ ACKNOWLEDGMENTS

The authors acknowledge the financial support provided by the Danish Hydrocarbon Research & Technology Centre (DHRTC) as part of the AWF.1 work package. The authors are also grateful to Total E&P Danmark for the provided drill core and produced oil samples.

■ REFERENCES

(1) Zhang, L.; Huang, X.; Fan, X.; He, W.; Yang, C.; Wang, C. Rapid fingerprinting technology of heavy oil spill by mid-infrared spectroscopy. *Environ. Technol.* **2019**, 1−9.

(2) Sánchez-Lemus, M. C.; Schoeggl, F. F.; Taylor, S. D.; Andersen, S. I.; Mapolelo, M. M.; Mahavadi, S. C.; Yarranton, H. W. Characterization of Heavy Distillation Cuts Using Fourier Transform Infrared Spectrometry: Proof of Concept. *Energy Fuels* **2016**, *30*, 10187−10199.

(3) Robin, P. L.; Rouxhet, P. G. Characterization of kerogens and study of their evolution by infrared spectroscopy: carbonyl and carboxyl groups. *Geochim. Cosmochim. Acta* **1978**, *42*, 1341−1349.

(4) Jewell, D. M.; Weber, J. H.; Bunger, J. W.; Plancher, H.; Latham, D. R. Ion-exchange, coordination, and adsorption chromatographic separation of heavy-end petroleum distillates. *Anal. Chem.* **1972**, *44*, 1391−1395.

(5) Aske, N.; Kallevik, H.; Sjöblom, J. Determination of Saturate, Aromatic, Resin, and Asphaltenic (SARA) Components in Crude Oils by Means of Infrared and Near-Infrared Spectroscopy. *Energy Fuels* **2001**, *15*, 1304−1312.

(6) Bhui, U. K.; Sanyal, S.; Saha, R.; Rakshit, S.; Pal, S. K. Steady-state and time-resolved fluorescence spectroscopic study of petroleum crudes in aqueous-surfactant solutions: Its implications for enhanced oil recovery (EOR) during surfactant flooding. *Fuel* **2018**, *234*, 1081−1088.

(7) Boczkaj, G.; Kamiński, M. Research on the separation properties of empty-column gas chromatography (EC-GC) and conditions for

simulated distillation (SIMDIS). *Anal. Bioanal. Chem.* **2013**, *405*, 8377−8382.
(8) Labedi, R. Use of production data to estimate volume factor, density and compressibility of reservoir fluids. *J. Pet. Sci. Eng.* **1990**, *4*, 375−390.
(9) Andersen, S. I.; Chandra, M. S.; Chen, J.; Zeng, B. Y.; Zou, F.; Mapolelo, M.; Abdallah, W.; Buiting, J. J. Detection and Impact of Carboxylic Acids at the Crude Oil−Water Interface. *Energy Fuels* **2016**, *30*, 4475−4485.
(10) Andersen, S. I.; Mahavadi, S. C.; Abdallah, W.; Buiting, J. J. Infrared Spectroscopic Analysis of the Composition of an Oil/Water Interfacial Film. *Energy Fuels* **2017**, *31*, 8959−8966.
(11) Mamonov, A.; Kvandal, O. A.; Strand, S.; Puntervold, T. Adsorption of Polar Organic Components onto Sandstone Rock Minerals and Its Effect on Wettability and Enhanced Oil Recovery Potential by Smart Water. *Energy Fuels* **2019**, *33*, 5954−5960.
(12) Norrman, K.; Sølling, T. I.; Ceccato, M.; Stamate, E.; Bovet, N.; Stipp, S. L. S. Chemical Composition and Structure of Adsorbed Material on Pore Surfaces in Middle East Reservoir Rocks. *Energy Fuels* **2018**, *32*, 11234−11242.
(13) Kasmaei, A. K.; Rao, D. N. Is Wettability Alteration the Main Cause for Enhanced Recovery in Low-Salinity Waterflooding? *SPE Reservoir Eval. Eng.* **2015**, *18*, 228−235.
(14) Leslie, Z. D.; Liu, S.; Puerto, M.; Miller, C. A.; Hirasaki, G. J. Wettability alteration and spontaneous imbibition in oil-wet carbonate formations. *J. Pet. Sci. Eng.* **2006**, *52*, 213−226.
(15) Standnes, D. C.; Austad, T. Wettability alteration in chalk. *J. Pet. Sci. Eng.* **2000**, *28*, 123−143.
(16) Jarrahian, K.; Seiedi, O.; Sheykhan, M.; Sefti, M. V.; Ayatollahi, S. Wettability alteration of carbonate rocks by surfactants: A mechanistic study. *Colloids Surf., A* **2012**, *410*, 1−10.
(17) Prabhakar, S.; Melnik, R. Influence of Mg^{2+}, SO_4^{2-} and Na^+ ions of sea water in crude oil recovery: DFT and ab initio molecular dynamics simulations. *Colloids Surf., A* **2018**, *539*, 53−58.
(18) Collins, I. R.; Couves, J. W.; Hodges, M.; McBride, E. K.; Pedersen, C. S.; Salino, P. A.; Webb, K. J.; Wicking, C.; Zeng, H. Effect of Low Salinity Waterflooding on the Chemistry of the Produced Crude Oil. *SPE Improved Oil Recovery Conference*, 2018; pp 1−17.
(19) Energistyrelsen, 2013. https://ens.dk/.
(20) Yang, Z.; Yang, C.; Wang, Z.; Hollebone, B.; Landriault, M.; Brown, C. E. Oil fingerprinting analysis using commercial solid phase extraction (SPE) cartridge and gas chromatography-mass spectrometry (GC-MS). *Anal. Methods* **2011**, *3*, 628.
(21) Alzaga, R.; Montuori, P.; Ortiz, L.; Bayona, J. M.; Albaigés, J. Fast solid-phase extraction-gas chromatography-mass spectrometry procedure for oil fingerprinting. *J. Chromatogr. A* **2004**, *1025*, 133−138.
(22) Nunn, S.; Nishikida, K. *Advanced ATR Correction Algorithm*; Thermo Electron Corporation, Application Note, 2003.
(23) Jiménez, O. P.; Pérez Pastor, R. M.; Segovia, O. E. An analytical method for quantifying petroleum hydrocarbon fractions in soils, and its associated uncertainties. *Anal. Methods* **2014**, *6*, 5527−5536.
(24) Jolliffe, I. T.; Cadima, J. Principal component analysis: a review and recent developments. *Philos. Trans. R. Soc., A* **2016**, *374*, 20150202.
(25) Lovatti, B. P. O.; Silva, S. R. C.; Portela, N. d. A.; Sad, C. M. S.; Rainha, K. P.; Rocha, J. T. C.; Romão, W.; Castro, E. V. R.; Filgueiras, P. R. Identification of petroleum profiles by infrared spectroscopy and chemometrics. *Fuel* **2019**, *254*, 115670.
(26) Wold, S.; Esbensen, K.; Geladi, P. Principal component analysis. *Chemom. Intell. Lab. Syst.* **1987**, *2*, 37−52.
(27) Malinowski, E. R. *Factor Analysis in Chemistry*, 3rd ed.; Wiley, 2002.
(28) Wojdyr, M. Fityk: a general-purpose peak fitting program. *J. Appl. Crystallogr.* **2010**, *43*, 1126−1128.
(29) OriginLab Corporation. *OriginPro*, Version, 2018: Northampton, MA, USA.
(30) Nielsen, J.; Poulsen, K. G.; Christensen, J. H.; Solling, T. I. Tracing Production with Analytical Chemistry: Can Oil Finger Printing Provide New Answers. *SPE Middle East Oil and Gas Show and Conference*, 2019; pp 1−17.
(31) Sundberg, J.; Feilberg, K. L. Characterization of heteroatom distributions in the polar fraction of North Sea oils using high-resolution mass spectrometry. *J. Pet. Sci. Eng.* **2020**, *184*, 106563.

https://dx.doi.org/10.1021/acsomega.0c04431
ACS Omega 2020, 5, 31753−31764